

Crystallization Thermodynamic and Kinetic Behaviors of Vitamin C in Batch Crystallizer*

CHEN Huiping (陈慧萍)* and WANG Jingkang (王静康)

School of Chemical Engineering, Tianjin University, Tianjin 300072, China

Abstract The bench-scale cooling crystallization for ternary solution of *L*-ascorbic acid (Vitamin C) was studied. The solid-liquid phase diagram of Vitamin C-water-ethanol system was obtained on the basis of differential scanning calorimeter (DSC) curves. The heat of crystallization of Vitamin C was calculated with the aid of quantitative analysis. According to the population balance equation under unsteady state, the rates of nucleation and growth were determined. The parameters of crystallization kinetics equations were estimated by regression of experimental data. Crystal morphology and size were determined with x-ray diffraction and TA II Coulter Counter.

Keywords Vitamin C, crystallization, thermodynamics, DSC, kinetics

1 INTRODUCTION

Crystallization is a complex multi-phase heat and mass transport process. The maximum yield of product crystal and the optimum operation conditions are determined by investigating crystallization thermodynamics. Crystallization kinetics decides the morphology and crystal size distribution (CSD) of product crystal and performance of crystallizer.

Vitamin C (*L*-ascorbic acid, $C_6H_8O_6$), an essential nutriment for health maintenance, plays an important role in pharmaceutical and food industries. Fedorova *et al.*^[1] found that the Vitamin C-water system is an eutectic system at the concentration $w = 11\%$ Vitamin C and at -3°C . A set of solubility data for Vitamin C in aqueous solution was measured by Apelblat and Manzurola^[2]. In the past years, however, only a few researchers have described the kinetic behavior of Vitamin C. Smirnov and his colleagues^[3] applied water and alcohol as solvent mixture in Vitamin C crystallization, and summarized a simple kinetics equation.

In this paper, the thermodynamic and kinetic behavior of Vitamin C crystallization in water-alcohol was studied in detail. The solid-liquid phase equilibrium diagram was determined with the aid of differential scanning calorimeter (DSC). An unsteady state method for measurement of nucleation and growth kinetics was employed. Combining the population balance model and mass balance equation, the expressions for nucleation and growth rates were formulated and the parameters were obtained by regression.

2 MATHEMATICAL MODEL

For a batch crystallization process in which crystal breakage and agglomeration are negligible and size is

independent of growth rate, the population balance equation is^[4]

$$\frac{\partial n}{\partial t} + G \frac{\partial n}{\partial L} = 0 \quad (1)$$

After Laplace transformation population density $n(L)$ expression becomes

$$\bar{n}(s, t) = \int_0^\infty n(L, t) \exp(-sL) dL \quad (2)$$

where s is the Laplace transform parameter. Therefore Eq. (1) can be transformed into

$$\frac{d\bar{n}(s, t)}{dt} + G[s\bar{n}(s, t) - n(0, t)] = 0 \quad (3)$$

Assuming that the initial size distribution for nuclei is $n(0, t)$, Eq. (3) reduces to

$$\frac{d\bar{n}(s, t)}{dt} + Gs\bar{n}(s, t) - B^0 = 0 \quad (4)$$

Converting Eq. (4) into the form of difference, Eq. (5) can be obtained

$$\frac{\Delta\bar{n}(s, t)}{\Delta t} = -Gs\bar{n}(s, t) + B^0 \quad (5)$$

Eq. (5) can be used to determine the kinetics rate since a plot of $\Delta\bar{n}(s, t)/\Delta t$ against $s\bar{n}(s, t)$ should yield a straight line with slope of $-G$ and intercept of B^0 .

The linear growth rate of crystal is also a function of supersaturation, expressed by

$$G = K_G \cdot \Delta C^g \quad (6)$$

or

$$G = K_g \exp(-E_G/RT) \Delta C^g \quad (7)$$

where K_G and k_g are growth rate coefficients, g is power exponent, ΔC is supersaturation, and E_G is the activation energy for growth.

The nucleation rate B^0 can be described by empirical power law

$$B^0 = K_B M_T^j G^i \quad (8)$$

or

$$B^0 = k_b \exp(-E_B/RT) N_p^l \Delta C^{n'} M_T^j \quad (9)$$

where K_B and k_b are nucleation rate coefficients, M_T is slurry density, G is linear growth rate, N_p is agitation speed, i , j , n' and l are exponents, and E_B is the activation energy for nucleation.

Combining Eqs. (5), (6) and (8), and using a multiple nonlinear regression, the kinetic parameters can be obtained.

3 EXPERIMENTAL

The samples for study of crystallization thermodynamics were prepared at different concentration of Vitamin C in solvent mixture in which the mass ratio of ethanol to water was kept constant to be 0.16. Thus the quasi-binary method was employed. The data of solid-liquid phase equilibrium were measured by differential thermal analysis with a TA300 DSC.

Fig. 1 shows the flow-sheet of kinetic experiments. The crystallizer is a jacketed glass vessel fitted with a draft-tube and up-flow propeller agitator. The slurry temperature was measured with alcohol thermometer and controlled at 43°C, 39°C, 30°C and 20°C respectively by water bath. Agitation speed was employed at 550 r·min⁻¹, 580 r·min⁻¹, 600 r·min⁻¹ or 730 r·min⁻¹ by agitation controller and voltage adjuster.

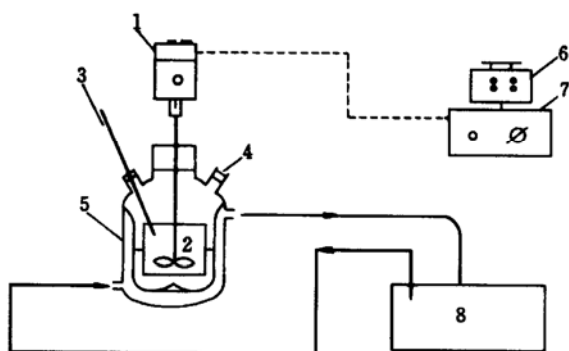


Figure 1 The flow-sheet of kinetic experiments for Vitamin C

- 1—electrical machinery; 2—impeller;
3—alcohol thermometer; 4—sample outlet;
5—crystallizer; 6—voltage adjuster;
7—agitation controller; 8—water bath

The solution of Vitamin C was prepared in solvent mixture (de-ionized water and ethanol) and the initial concentration was measured. The crystallization

process was carried out by cooling. After nucleation occurred, the samples were withdrawn to determine CSD by TAIL Coulter Counter and the concentration of solution by iodimetry. At the same time, the temperature and volume of solution were recorded.

In the experiments the effects of supersaturation, slurry density, agitation and temperature on nucleation and growth rates were investigated.

4 RESULTS AND DISCUSSION

4.1 Solid-liquid phase equilibrium of Vitamin C crystallization system

Under the condition with normal pressure and a constant mass ratio of ethanol to water, the crystallization thermodynamics for this three-component system was studied using quasi-binary method and the phase diagram can be plotted in a plane figure. When Vitamin C concentration in solvent mixture was changed, DSC curves for different Vitamin C concentration were obtained and analyzed.

It was found that the system was not a simple eutectic one. According to the peak temperatures of DCS curves at different concentrations of Vitamin C, the phase diagram of quasi-binary system was drawn in Fig. 2 (marked with ●). For comparison the phase diagram of Vitamin C-water reported in literature^[1,2] was also presented (marked with ○).

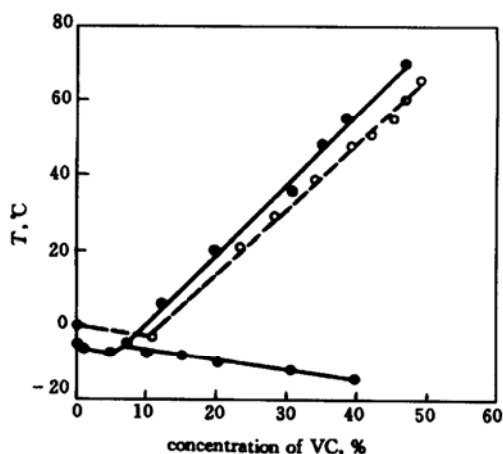


Figure 2 The solid-liquid phase diagram of Vitamin C crystallization system

- Vitamin C-water-ethanol system, where the mass ratio of EtOH to H₂O is 0.16;
○ Vitamin C-water system^[1,2]

The liquidus line has a minimum with the concentration of 5% (w) and temperature at -7.3°C for the Vitamin C-water-ethanol system, and intersects the solidus line at a point with the concentration 7.0% (w) and temperature -5°C, while in Vitamin C-water system the eutectic concentration is 11% (w) at -3.5°C.

Thus we can conclude that the added ethanol decreases the solubility of Vitamin C in aqueous solution and is beneficial to increase the yield of Vitamin C crystals.

When the mass ratio of ethanol to water decreased (EtOH/H₂O=0.096; 0.064), at the same concentration of Vitamin C, the temperature of solidus line increased to different extent.

When the system was cooled below -5°C, not only Vitamin C but also some solvate was crystallized, which was verified by experimental observation. Therefore in Vitamin C batch cooling crystallization the final temperature should be controlled above -5°C, so that the larger increase in the yield can not merely depend on lowering the crystallization final temperature, but lessening the solvent amount by vacuum evaporation.

With the aid of quantitative analysis and the endothermic peak area of DSC curve, the heat of crystallization of Vitamin C can be measured: $\Delta H = 175 \text{ J}\cdot\text{g}^{-1} = 31 \text{ kJ}\cdot\text{mol}^{-1}$.

4.2 The crystal morphology of Vitamin C

The nature and habit of single crystal of *L*-ascorbic acid have been discussed by Cox & Goodwin^[5] and Hvoslef^[6]. The present investigation also determined the structure by x-ray diffraction with Enraf-Nonius crystal angle-4 diffraction (CAD-4). A survey of the different results is given in Table 1.

Table 1 The parameters of unit cell

	<i>a</i> , nm	<i>b</i> , nm	<i>c</i> , nm	β , (°)
Cox & Goodwin	1.695	0.632	0.638	102.30
Hvoslef	1.7299	0.6353	0.6411	102.11
present study	1.7101	0.6349	0.6393	99.26

Vitamin C crystals belong to monoclinic crystal system, P₂₁ space group. The structures of unit cell and molecule are shown in Figs. 3 and 4 respectively.

From the intermolecular bonding system it can be seen that the cell of Vitamin C has greater density of hydrogen bonds along *y* axis or *z* axis of unit cell than along *x* axis. Combining with its Miller-indices reported by Bodor and Dodony^[7], the face (010) is a polar face comparing with the face (100) and their face growth rate are different. In the experiments of cooling crystallization, if the cooling rate is very high, the solution supersaturation is large and the relative growth rate for different crystal faces will also increase largely, so that some crystal faces will disappear and the habit of Vitamin C crystals is usually to be platy. If we apply an appropriate cooling condition in crystallization, the difference of face growth rates can be reduced, so that the habit of crystals changes from a plate-like form to a more prismatic one (Fig. 5).

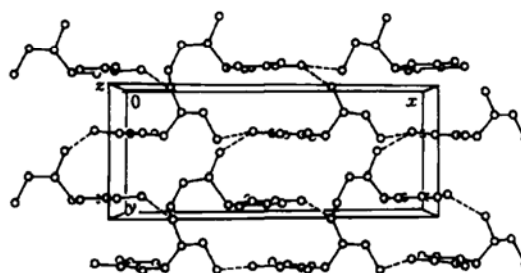


Figure 3 Cell structure of Vitamin C by x-ray diffraction

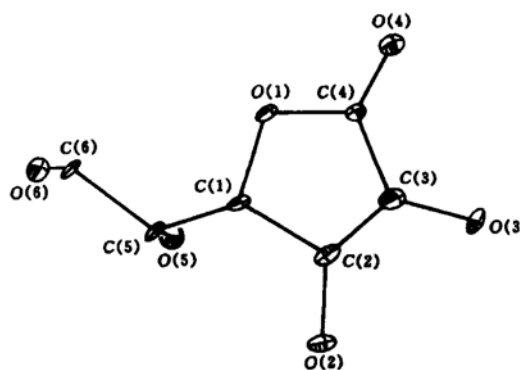


Figure 4 The molecular structure of Vitamin C



Figure 5 Vitamin C crystals

4.3 Nucleation and growth rates for Vitamin C crystallization

On the basis of experimental data, the supersaturation ΔC , slurry density M_T of samples, the nucleation and growth rates B^0 and G were determined. The growth rate decreased as the solution supersaturation decreased, but the slurry density increased gradually, so that the nucleation rate had a maximum. Even at low levels of supersaturation, the nucleation rate was high, so the fines were inevitably present in the product. On the basis of sample size analysis, the value of growth rate is about 10^{-8} — $10^{-7} \text{ m}\cdot\text{s}^{-1}$, which

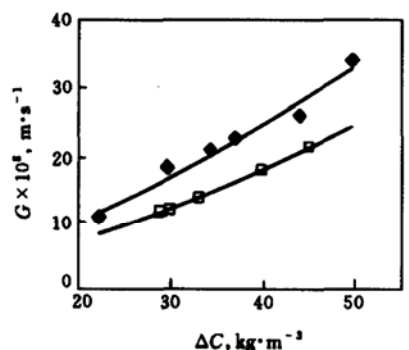
is determined as linear growth rate, dL/dt , while that of nucleation rate is about $10^9 \text{ No} \cdot \text{m}^{-3} \cdot \text{s}^{-1}$.

4.4 Effects of agitation speed and temperature on nucleation and growth rates

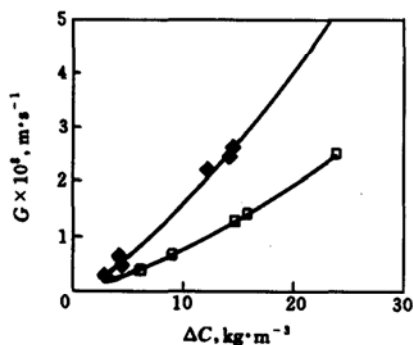
4.4.1 Effect of agitation and temperature on growth rate

(1) Temperature

Fig. 6 shows that growth rate largely rises as the temperature increases. It is contributed that the growth process is an endothermal process.



(a) \blacklozenge 316.15 K; \square 312.15 K



(b) \blacklozenge 303.15 K; \square 293.15 K

Figure 6 Growth rate versus supersaturation at different temperatures

(The agitation speed at $550 \text{ r} \cdot \text{min}^{-1}$)

(2) Agitation

The growth rate constant K_G should increase as the agitation speeds up from 550 to $720 \text{ r} \cdot \text{min}^{-1}$ (Fig. 7). The growth of crystal includes two steps, solute diffusion and surface reaction. Stirred at a low speed, the process is controlled by diffusion. While the stirring speed is raised, higher mass transfer rate in the crystallizer is achieved. Under such circumstances, the transport coefficient increases. Thus the process of crystallization controlled by diffusion changes to be controlled by surface reaction. Therefore the minimum growth rate may exist. However in our experiments, the agitation speed only changed in limited range, so the phenomenon cannot be observed.

4.4.2 Effect of agitation speed and temperature on nucleation rate

(1) Temperature

As shown in Fig. 8, the increase in temperature can promote secondary nucleation process in vitamin C crystallization, because the solute molecules must overcome the molecular forces to form nuclei.

(2) Agitation speed

Adding the input energy, the contact frequency increases and the secondary nucleation rate is larger. Thus the agitation speed N_p exerts a great influence on the nucleation rate. However, since the regressed kinetic parameters have a certain error, if given values of the exponents are adopted, the effect of agitation on nucleation is not clear when all experimental points were plotted in the same figure.

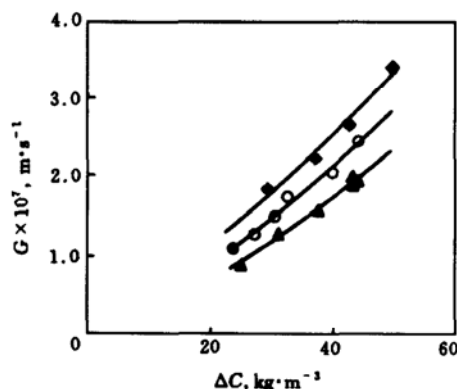


Figure 7 Growth rate versus supersaturation at different agitation speeds

(The temperature at 316 K) $N, \text{ r} \cdot \text{min}^{-1}$:
 \triangle 730; \circ 600; \blacklozenge 550

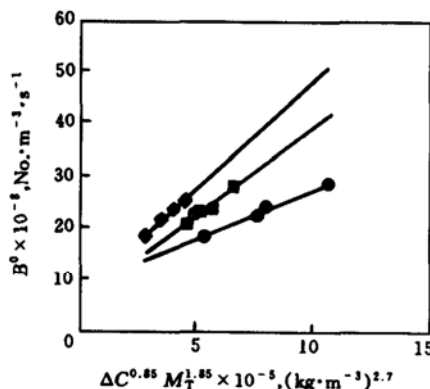


Figure 8 The effect of temperature on secondary nucleation

(The agitation at $550 \text{ r} \cdot \text{min}^{-1}$)
 $T, \text{ K}$: \blacklozenge 316; \blacksquare 312; \bullet 293

Based on the results, the crystallization kinetics equations of Vitamin C were finally formulated and the parameters were obtained by regression: linear growth rate

$$G = k_g \exp(-E_G/RT) \Delta C^g$$

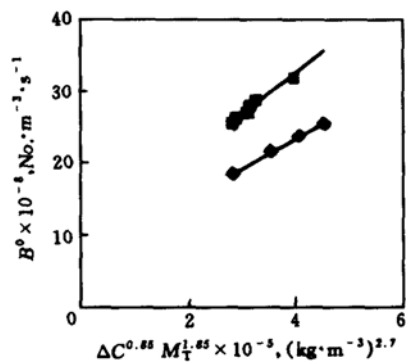
$$k_g = 0.44, E_G = 5.2 \times 10^4 \text{ J} \cdot \text{mol}^{-1}, g = 1.4 \quad R' = 0.97$$

nucleation rate

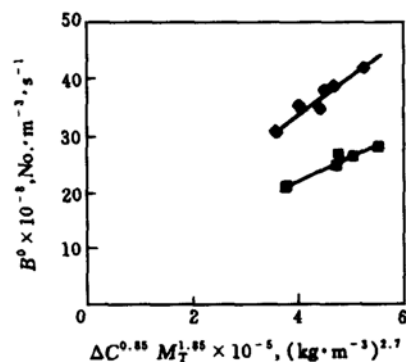
$$B^0 = k_b \exp(-E_B/RT) N_p^l \Delta C^b M_T^j$$

$$k_b = 7.2E + 07, E_B = 3.3 \times 10^4 \text{ J} \cdot \text{mol}^{-1},$$

$$l = 1.5, b = 0.85, j = 1.85 \quad R' = 0.87$$



(a) $N, \text{r} \cdot \text{min}^{-1}$: ■ 600; ◆ 550



(b) $N, \text{r} \cdot \text{min}^{-1}$: ■ 730; ◆ 580

Figure 9 The effect of agitation on secondary nucleation (The temperature at 316 K)

in which experimental supersaturation ΔC ranges from 2 to 67 $\text{kg} \cdot \text{m}^{-3}$, and the slurry density M_T changes between 129 and 457 $\text{kg} \cdot \text{m}^{-3}$.

The activation energy of growth is 52 $\text{kJ} \cdot \text{mol}^{-1}$, and that of nucleation is 33 $\text{kJ} \cdot \text{mol}^{-1}$.

Thus the effect of temperature on growth is stronger than that on nucleation, and the data of activation energy is coincident with the heat of crystallization.

5 CONCLUSIONS

The system of Vitamin C-water-ethanol is not a simple eutectic system. The liquidus line has a minimum with the concentration of 5% and temperature

at -7.3°C for this system, and intersects the solidus line at a point with the concentration 7.0% and temperature -5°C . The heat of crystallization of Vitamin C was calculated to be 31 $\text{kJ} \cdot \text{mol}^{-1}$.

The parameters in crystallization kinetics equations can be obtained by regression. And the activation energy of growth and nucleation processes was obtained to be 52 $\text{kJ} \cdot \text{mol}^{-1}$ and 33 $\text{kJ} \cdot \text{mol}^{-1}$ respectively. This study provides the basis for modeling the cooling crystallization of Vitamin C.

NOMENCLATURE

a, b, c	axial lengths of unit cell, nm
B^0	nucleation rate, $\text{No.} \cdot \text{m}^{-3} \cdot \text{s}^{-1}$
ΔC	supersaturation, $\text{kg} \cdot \text{m}^{-3}$
E	activation energy, $\text{J} \cdot \text{mol}^{-1}$
G	linear growth rate, $\text{m} \cdot \text{s}^{-1}$
g	exponent
ΔH	heat of crystallization, $\text{J} \cdot \text{mol}^{-1}$
i, j, l	exponents
K_B, k_b	nucleation rate coefficient
K_G, k_g	growth rate coefficient
L	crystal size, m
M_T	slurry density, $\text{kg} \cdot \text{m}^{-3}$
N_p	agitation speed, $\text{r} \cdot \text{s}^{-1}$
n	population density, $\text{No.} \cdot \text{m}^{-4} \cdot \text{s}^{-1}$
$\bar{n}(s, t)$	the form of n in Laplace transform
n'	exponent
R	gas constant, $8.314 \text{ J} \cdot \text{mol}^{-1} \cdot \text{K}^{-1}$
R'	coefficient of relation
s	Laplace transform parameter
T	temperature, K or $^\circ\text{C}$
t	time, s
β	angle between a and b axis, ($^\circ$)

REFERENCES

- 1 Fedorova, R. V., Fedorov, P. I., Shvedov, Yu. P., *Zh. Prikl. Khim.*, **44** (9), 2039 (1971).
- 2 Apelblat, A., Manzurola E., *J. Chem. Thermodyn.*, **21** (9), 1005 (1989).
- 3 Smirnov, N. Yu., Strel'tsov, V. V., et al., *Khim. Khim. Tekhnol.*, **18** (1), 126 (1975).
- 4 Randolph, A. D., Larson, M. A., *Theory of Particulate Process*, Academic Press, New York (1971).
- 5 Cox, E. G., Goodwin, T. H., *J. Chem. Soc.*, 769 (1936).
- 6 Hvoslef, J., *Acta. Crystallogr., Sect. B***24**, 23 (1968).
- 7 Bodor B., Dodony I., *Hungarian J. Ind. Chem.*, **23**, 289 (1995).